NASA Technical Paper 1438

Operating Characteristics of a Cantilever-Mounted Resilient-Pad Gas-Lubricated Thrust Bearing

Zolton N. Nemeth

APRIL 1979

NASA

NASA Technical Paper 1438

Operating Characteristics of a Cantilever-Mounted Resilient-Pad Gas-Lubricated Thrust Bearing

Zolton N. Nemeth
Lewis Research Center
Cleveland, Ohio

National Aeronautics
and Space Administration

**Scientific and Technical
Information Office**

1979

SUMMARY

A previously analyzed resilient-pad gas thrust bearing consisting of six pads mounted on cantilever beams was tested experimentally to determine its operating characteristics. The film thickness between the bearing pad and the runner and the bearing friction were obtained and compared with theory. The bearing had a 10-centimeter outside diameter and a 5-centimeter inside diameter. It was run in air at a constant thrust load of 74 newtons which resulted in a unit load of 16.8 kilonewtons per square meter. Test speed ranged up to 17 000 rpm.

The cantilever-mounted-pad test bearing performed well and was equal to that of a Rayleigh step bearing of approximately the same unit load. The experimental film thickness was less than that predicted by theory. Bearing friction torque was greater than that predicted by theory but was less than twice the predicted value.

INTRODUCTION

Gas-lubricated bearings under certain environmental conditions offer the only possibility of rotor bearing support without having a highly complex bearing lubrication system that uses a conventional oil lubricant. These environmental conditions are extreme temperature, long life, high speed, and localized loading.

The many types of gas bearings with their advantages and disadvantages have been thoroughly discussed in the literature (e.g., ref. 1). The types of gas bearings fall into the main classes of rigid geometry, segmented rigid geometry, and foil bearings. Since flexibility or a conformable bearing surface is a desirable feature to avoid localized loading, foil bearings have been used recently in many applications for rotor support (refs. 2 and 3). Some of the important characteristics of foil bearings are their simplicity and low mass and inertia which enhances the stability of operation.

Whereas a foil bearing lends itself to the journal geometry efficiently, it does not to the thrust bearing geometry. In the foil journal bearing the radial load can be supported by a well-defined gas film which is naturally formed by foil wrapped around the journal. In the thrust bearing, however, the film wedge has to be formed by specialized foil support schemes which are inadequate to the formation of an undistorted fluid film shape (refs. 1 and 4).

There is a need for an efficient gas thrust bearing (ref. 1). Investigators have approached the problem two ways: (1) by combining a high load-capacity spiral groove pattern on a flexible membrane and supporting this membrane parallel with the runner with a distributed stiffness support of plate spring arrays, and (2) by mounting rigid load carrying plates (such as pads) on resilient foil annular beams (ref. 5). Both configurations performed in a satisfactory manner over the operating range. However, the resilient-mounted-pad gas thrust bearing exhibited surface rubbing at low loads and high speeds (ref. 5). It was found through a subsequent analysis that the load capacity is maximized whenever the pad tilt results in a uniform minimum film thickness along the pad trailing edge (ref. 6). The annular beams of reference 5 did not give a uniform minimum film thickness along the pad trailing edge.

A uniform minimum film thickness along the trailing edge in a pad could be obtained by making the pad flexible as in reference 7. However, this scheme lends itself better to highly loaded applications with oil-lubricated bearings than in lightly loaded applications with gas lubrication. A new type of resilient-pad gas thrust bearing was described and analyzed in reference 8. The bearing has rigid pads mounted on flexible cantilever beams. The design of the cantilever-mounted resilient pad is such that a uniform minimum film thickness is obtained along the trailing edge of the pad. The bearing was optimized for operation at a given load and speed, and the operating characteristics were determined for a range of speeds and loads.

The present study is a continuation of this earlier investigation. The objective was to determine the feasibility of the cantilever-mounted resilient-pad gas thrust bearing by fabricating and experimentally evaluating the cantilevered thrust bearing at one load and over a limited speed range and by comparing the experimental results with theory. Feasibility of this design concept would be determined from the friction torque and pad film thickness data produced in the test thrust bearing and by comparison to Rayleigh step bearings.

The tests were performed with a thrust bearing with six pads. Each pad was mounted on a 4.0-centimeter-long cantilever beam. The bearing had a 10.0-centimeter outside diameter and a 5.0-centimeter inside diameter. Speed was varied to 17 000 rpm. The thrust load was a constant 74 newtons or a load pressure of 16.8 kilonewtons per square meter except at startup and shutdown when the load was removed from the pads and supported by an auxiliary pressurized thrust bearing. Ambient air at 297 K was used as the lubricant.

APPARATUS

Test Thrust Bearing

The cantilever-mounted resilient-pad gas thrust bearing is shown in a schematic drawing in figure 1 and in a photographic view in figure 2(a). The thrust bearing consists of six pads mounted at the end of resilient, metallic, cantilever beams which are mounted on a support plate. The pad and beam were cut from one piece of metal to eliminate any mechanical load deflection hysteresis since the minimum film thickness to be measured was expected to be small, about 0.013 millimeter. The mating runner is shown in figure 2(b). It is a single large disk with a smaller inner disk.

Bearing Design

The design of the cantilever-mounted resilient-pad gas thrust bearing was reported in reference 8. A bearing design example was presented for the bearing thrust load (which was the fixed weight of the shaft) of 74 newtons and a speed of 34 000 rpm.

A six-pad gas-lubricated bearing having the following dimensions was designed for the operating conditions chosen:

Outer radius of pad, r_o, cm	5
Inner radius of pad, r_i, cm	2.5
Angular extent of pad, β, deg	45
Ambient pressure, p_a, N/m^2	1×10^5
Dynamic viscosity of gas, μ, $N\text{-sec}/m^2$	1.86×10^{-5}
Young's modulus of beam material, E, N/m^2	2.1×10^{11}
Beam width, b, cm	2
Beam thickness, t, mm	3.6
Beam length, ℓ, cm	4

The pad and beam configuration took on an offset shape to accommodate the intertwining assembly of the six pads and beams (fig. 3). The pad is made integral with the beam. The pad and the mounting end of the beam were made thicker than the beam to preclude deflection in these sections under load.

The test thrust bearing material was hardened 17-4 PH stainless steel for the pad beam and hardened M-50 steel for the mating runner. The bearing surfaces, pads, and runner were coated with plasma-sprayed chromium oxide (Chromia, Cr_2O_3) for wear prevention. The Cr_2O_3 coating was approximately 80 micrometers thick after grinding.

The bearing surfaces were finish lapped flat to within 2.5 micrometers. The pad surfaces were initially manufactured (with the Cr_2O_3 coating) to close tolerance so that just a small amount of lapping would be required at assembly to bring the surfaces of the six pads into one flat plane within 2.5 micrometers. The pad surfaces of the thrust bearing assembly were lapped with the light weight of the bearing assembly acting on the bearing.

Test Apparatus

The test apparatus used in this investigation is shown in figure 4. It is fully described in reference 9. Briefly, it consists of a vertically oriented rotor, which is supported by two identical tilting pad journal bearings, and the test thrust bearing at the lower end of the rotor. The rotor is driven by a small air turbine mounted on the upper end of the rotor. Each journal bearing has three pads, and each pad is supported on a pivot. One of the pivots in each journal bearing is mounted on a low spring rate flexure (7.6×10^5 N/m) to accommodate radial growth of the rotor and to keep the critical speed and associated bearing loads low. The two journal bearings are 28 centimeters apart.

The test rig had no capability of varying the test thrust bearing load, which was 74 newtons - the fixed weight of the shaft. The unit loading on the thrust bearing pads was 16.8 kilonewtons per square meter.

An externally pressurized shaft lift bearing was incorporated into the thrust test bearing for startup and shutdown (fig. 5). The lift bearing raised the shaft and rotor about 0.3 millimeter off the test bearing pad surfaces and at the same time floated the shaft on a pressurized film of air. Stop screws in the lift bearing limited the lift height and prevented the shaft from being pushed against the drive turbine at the upper end of the shaft. After the thrust bearing was brought up to speed for self-acting capability of the test thrust bearing the lift bearing pressure was shut off. The lift bearing retracted and allowed the shaft weight to be supported by the thrust bearing.

The test thrust bearing was supported on a self-alining gimbal and a nonrotating externally pressurized bearing (fig. 6) so that the test bearing friction torque could be measured accurately.

Instrumentation

The test thrust bearing was instrumented with capacitance- and inductive-type probes to measure the film thickness and the beam deflection, as well as to monitor the bearing and pad motions. Three 0.13-millimeter-range capacitance probes were

mounted in one pad with epoxy, as shown in figure 7, for the film thickness measurement. The three inductive probes were mounted in the bearing pad support plate to measure the deflection of three individual cantilever beams. The layout of these probes in the thrust bearing is shown in figures 1 and 8. Two other capacitance probes were installed below the thrust bearing support plate 90^{o} apart to monitor the thrust bearing plate motion in the gimbal to assure proper motion of the thrust bearing.

The shaft radial motion was monitored. Two radial capacitance probes, each having a 0.25-millimeter range, were mounted outboard of each journal bearing.

Each probe was calibrated before being installed in the test apparatus and the test bearing. The pad probes were calibrated against a chrome oxide plated surface. A high temperature epoxy was used to mount the capacitance probes in the test bearing pad to prevent yielding of the adhesive during operation due to temperature and film air pressure (the temperature and pressure were not expected to be appreciably great). The three capacitance probes were set about 0.05 millimeter below the pad surface.

Thrust bearing torque was measured with an unbonded strain gage transducer that was attached to the outer diameter of the pressurized support bearing. The bearing torque was measured accurately because the bearing support floated without friction on pressurized air.

Shaft speed was measured by a magnetic pickup and indicated on an electronic counter. The pickup faced six equally spaced shallow holes machined on the diameter of the shaft. This induced a signal in the magnetic probe and produced a reading in rpm on the counter. The shaft speed was controlled by an electronic controller which regulated the turbine air supply.

The data were recorded and displayed on a cathode ray oscilloscope. Because of the many data channels, a 14-channel FM tape recorder was used for permanent record and readout after the completion of the experiment.

Air Supply System

Service air (8.3×10^{5} N/m^{2} supply) was used to drive the turbine and to pressurize the hydrostatic air bearings through appropriate pressure regulators. The air was cleaned to remove moisture, oil vapor, and solid particles. Ambient room air was the lubricant for the self-acting cantilever-mounted-pad test thrust bearing. The temperature of the room was maintained at 297 K.

PROCEDURE

The capacitance pad probe signals and the inductive cantilever beam deflection probe signals were zeroed electronically. The inductive probe signal was zeroed when the beam deflection was zeroed by removing the shaft weight from the test thrust bearing. The capacitance probe signal was zeroed at zero film thickness between the pad and runner surfaces. This proved to be somewhat difficult because of the flexibly mounted pad on the cantilever beam and the requirement to maintain the pad surface parallel with the runner surface.

To get zero bearing film thickness, that is, contact between the pad and runner, and still maintain parallelism of the mating surfaces requires very light loading. Heavier loading starts to incline the pad with the runner. The test shaft is first just lifted off the test thrust bearing and held with a bracket. The test bearing is then lifted toward the runner in stages by pressurizing the externally pressurized bearing support. The output voltages from the film thickness and the beam deflection probes are recorded and plotted. Zero film thickness is at the knee of the curves. Output voltages from the pad capacitance at this point are bucked down to zero with a bucking voltage source.

The friction torque sensor output was checked to see if it gave the correct output with a 100-gram calibrating weight attached to the outer diameter of the pressurized support bearing to load the torque sensor. Attached instrumentation leads and air feed tubing were hung in a neutral position so as not to influence the bearing torque system.

To start a test the thrust bearing shaft and runner were lifted off the test thrust bearing pads with the lift bearing by pressurizing it with air. The bearing was brought up to a speed (approximately 7500 rpm) sufficient to have self-acting or hydrodynamic operation. With the test bearing at speed, external pressurization to the lift bearing was rapidly shut off with a solenoid valve, thereby dropping the shaft weight and the mating runner on the thrust bearing stator. Shaft speed was varied and bearing torque and pad clearance and beam deflection were obtained.

To stop the test the shaft was allowed to coast down to about 7500 rpm before the shaft weight was removed from the test thrust bearing by pressurizing the lift bearing. The shaft was then allowed to coast down to zero speed while floating on a pressurized film of air.

Testing was conducted as detailed but a few tests were made with the gimbal self-alining section removed and the thrust bearing clamped rigidly. The mating thrust bearing surfaces were carefully set to be parallel. The bearing then was tested to see if the flexible beam design was adequate for bearing alinement during operation and to see if higher speeds could be run without the self-alining gimbal support.

Some tests were made to determine the touchdown speed at which contact is just made between the bearing mating surfaces. Touchdown speed was taken as the speed at which the minimum bearing torque was reached. The lift bearing was activated at this point to separate the surfaces to minimize rubbing damage.

RESULTS AND DISCUSSION

Tests were performed to obtain film thickness and bearing friction torque measurements on a cantilever-mounted-pad air thrust bearing. Comparison was made between the experimental data and the previously reported theoretical data. The test thrust bearing had six pads. It was operated at a fixed load of 74 newtons (load pressure, 16.8 kN/m^2) and speeds to 17 000 rpm. The bearing was operated with air as the lubricant.

The results of the tests and comparisons are presented in figures 9 to 21.

Test Results

Beam deflection. - The deflection of three beams of a six-pad bearing is shown in figure 9. The three beams did not deflect the same amount as was expected. The cause is not known as no malfunction could be found in the instrumentation. It is to be remembered that the bearing was final lapped as an assembly and that the faces of the pads were checked for coplanar accuracy. The bearing is not of a self-leveling construction and some differences in the deflection among the beams are to be expected.

Figure 9 shows that there is an influence of speed on beam deflection up to a speed of about 14 000 rpm. The beam deflection remains constant with speed thereafter to about 17 000 rpm. All three beams deflect more initially than later on with increasing speed. Beam 2, which was deflected least at zero speed, showed greater change in deflection when the rotor was started, probably because the gas film helps to equalize the load among the pads. The increase in deflection with speed is the same for all three beams from 8000 to 14 000 rpm. An increase in beam deflection with speed can be explained by a change in the loading of a pad with speed. With an increase in speed the center of pressure moves to increase the lever arm (ref. 10). At zero speed the pad is loaded by the mating runner at the trailing edge. When the bearing is operating the load on the pad is acting at the center of pressure of the gas film and the center of pressure moves away from the trailing edge to increase the lever arm. The theoretical beam deflection (which can be obtained from ref. 8) is shown in figure 9. The theoretical beam deflection is constant with speed and is approximately the same magnitude as the deflection of beam 2.

Bearing torque. - Thrust bearing torque as a function of rotor speed is shown in figures 10 to 12 for three bearing assemblies and two mount modes. Assemblies one and three were gimbal mounted. Assembly two was clamp mounted. All three bearing assemblies exhibited approximately the same friction torque characteristics with speed. Friction torque increased with speed at about the same rate. At the transition of operation at start from the externally pressurized lift bearing to the hydrodynamic pad bearing or vice versa at stop there is a momentary high friction torque pulse. The momentary pulse is due to the edge contact of the nonalined free bearing with the mating runner. At first the bearing was allowed to coast to a complete stop (figs. 10 and 11). Then for later runs the coastdown under hydrodynamic conditions was only allowed to proceed as long as torque decreased with speed. When torque started to rise the lift bearing was activated (fig. 12) to lift the runner from the bearing pads to minimize surface damage from rubbing. The speed at minimum friction torque was about 3800 to 4000 rpm. The minimum friction torque was 0.56 newton-centimeter (fig. 10).

Effect of bearing mount. - The cantilever-mounted pad thrust bearing was run initially with a gimbal self-alining bearing mount because good alinement is required with a gas bearing. However, it was thought that the cantilever-flexure-mounted pad would provide sufficient alinement so that the additional alinement of a gimbal would not be required. With simplification also in mind, the gimbal mount was eliminated and the bearing support plate was clamped.

The clamped bearing ran well but not as well as with the gimbal mount. The starting speed for hydrodynamic operation was higher for the clamped bearing. This can be seen from the coastdown data. The minimum speed before rubbing is approximately 6000 rpm for the clamped bearing and approximately 4000 rpm for the gimbal-mounted bearing. Because the speed was not high enough at the start before hydrodynamic operation was attempted for the clamped bearing mount, the bearing torque was high and the lift bearing had to be reapplied to reach a higher speed (fig. 11).

At the upper speed the clamped bearing did not operate as well as the gimbal-mounted bearing. The gimbal-mounted bearing was limited to approximately 17 000 rpm before the high amplitude of thrust bearing instability caused an increase in bearing torque and the likelihood of rubbing. The clamped bearing mount limited the thrust bearing to an upper speed of approximately 14 000 rpm before the instability set in and bearing torque increased (fig. 11). Critical speed amplitude was noticed at 7000 and 11 000 rpm with the self-alining gimbal assemblies; this amplitude was increased at about 7000 rpm, but it was absent at about 11 000 rpm for the clamped bearing mount.

The clamped bearing was run under an adverse condition of high bearing torque to attempt to go through the instability and reach higher speeds. The effect of this type of

operation is shown in figure 13. The Cr_2O_3 surface coating on the pads wore so thin for the clamped bearing mount that light is reflected from the base metal in the light areas. The coating was originally thinner than desired because of reassembly and lapping. The most heavily worn surfaces are on five pads retained from the first assembly of the bearing. The second assembly interchanged one pad with an instrumented pad. The instrumented pad does not show as much surface wear as to the other five pads. For comparison a new bearing assembly is shown in figure 14.

Film thickness. - Film thickness as a function of rotor speed is shown in figures 15 and 16 for bearing assembly three for two runs. This bearing was gimbal mounted. No film thickness data were obtainable from the other bearing with the clamped bearing mount because of bearing wear.

Runs one and two show increasing film thickness with increasing speed in the speed range tested from about 4000 to about 17 000 rpm. Figure 15 shows both increasing and decreasing speed runs. Figure 16 shows only decreasing speed. Probe 11 in the first run indicates a film thickness above that of probe 8 which was near the trailing edge of the pad. In the second run the film thickness of probe 11 dropped in magnitude and was about equal to that of probe 8; however, the film thickness of probe 8 increased in the second run over that of the first run. The trailing edge surface is most vulnerable to wear even in the static condition with the weight of the shaft on the bearing. Wear of the surface coating would tend to smooth out the surface and fill the somewhat porous Cr_2O_3 surface, thereby increasing the film thickness.

Comparison of Test Results with Theory

Film thickness. - The experimental minimum film thickness as measured with probe 8 is compared with the theoretical minimum film thickness from reference 8 over the speed range to about 17 000 rpm in figure 17. For the various runs of bearing assembly three it can be seen that the experimental minimum film thickness is low for the first run but becomes better in comparison with theory for the next two runs. In the third run the experimental film thickness is about the same as the theoretical film thickness. The improvement in comparison in the experimental and the theoretical film thickness is probably because of the wear or polishing of the Cr_2O_3 porous surface of the bearing pads and the runner. With a smoother bearing surface on the film the thickness is greater.

The experimental recorded film thickness for the three capacitance probes in a pad is shown with the theoretical film thickness in figures 18 and 19. The theoretical minimum film thickness is obtained from that reported in reference 8 (fig. 7). The theoretical film thickness in the other capacitance probe locations is obtained from the

slope in figure 4 (ref. 8). Both film thicknesses at probe locations 8 and 11 were lower than that predicted by theory for the first run (fig. 18). For the second run probe 8 location the film thickness increased and was almost that predicted by theory (fig. 19), but the film thickness at probe location 11 was approximately that of probe location 8 and was not plotted. The film thickness at probe location 13 near the leading edge of the pad was nearly that predicted by theory for both the first and second runs.

Friction torque. - Comparison of the measured bearing friction torque with that of theory is shown in figure 20. The friction in figure 11 of reference 8 is for one pad and has to be multiplied by 6 to obtain the theoretical friction torque for a bearing with six pads. The measured friction torque was greater than that predicted by theoretical analysis for all three bearing assemblies but not more than twice the value predicted. Since the measured film thickness was less than theoretical, the friction torque is expected to be greater than that predicted by theory.

The values of friction torque for the three bearing assemblies increased with speed in the speed range tested up to about 17 000 rpm. The torque increase with speed paralleled that predicted by theory. The first bearing assembly produced the lowest bearing torque. The first bearing assembly was not instrumented with capacitance pad probes and the bearing torque was obtained first. The other two bearing assemblies had pad probes, and runs were made with them to obtain film thickness data first. Normal running might have worn the bearing surfaces to produce higher friction torque later. This is not the case with the third assembled bearing with three runs where friction torque was about the same for each run.

General Comments

The cantilever-mounted-pad gas thrust bearing performed about as well as a Rayleigh step thrust bearing that was approximately the same size, had about the same surface area, and was run in the same test rig under identical conditions with a gimbal mount (ref. 9). The Rayleigh step bearing had an outside diameter of 8.9 centimeters and an inside diameter of 5.4 centimeters; the cantilever-mounted-pad gas thrust bearing had an outside diameter of 10 centimeters and an inside diameter of 5 centimeters. The touchdown speeds on coastdown were about the same for both bearings in the 3700 to 4000 rpm range. The minimum theoretical film thickness was about the same also (see fig. 21). Film thickness was not measured for the Rayleigh thrust bearing.

The dynamic motion of the cantilever-mounted resilient-pad thrust bearing was also similar to the dynamic motion of the previously investigated Rayleigh step thrust bearing. This fact limited the upper limit of speed to 17 000 rpm in this investigation. The thrust bearing developed a large amplitude instability motion if operated beyond

17 000 rpm. Motions were small and controlled for speeds below 17 000 rpm. Future work for gas thrust bearings needs to be directed at the rotor bearing dynamics and specifically at the reduction of the mass of the thrust bearing assembly and the introduction of damping into the bearing assembly.

SUMMARY OF RESULTS

A cantilever-mounted resilient-pad gas-lubricated thrust bearing was run to determine the operating characteristics of this type of bearing experimentally. The bearing was run in air with a constant thrust load of 74 newtons over a speed range to 17 000 rpm. The film thickness between the pad and the runner and the bearing friction torque were measured. These were compared with those obtained from theory. The thrust bearing had six pads. The outside diameter was 10 centimeters and the inside diameter was 5 centimeters. The unit loading on the bearing pads was 16.8 kilonewtons per square meter. The following results were obtained:

1. Feasibility of the cantilever-mounted resilient-pad bearing was shown by a demonstrated performance that was the same as that of a Rayleigh step bearing carrying approximately the same unit load. The touchdown speed on coastdown was approximately the same for both bearing types between 3700 and 4000 rpm.

2. The measured minimum film thickness between the pad and the runner was initially less than that predicted by theory. The difference between the measured clearance and that of theory decreased with successive runs. The measured film thickness at the leading edge of the pad was approximately that predicted by theory. The porous surface coating on the bearing could account for the lower film thickness.

3. The experimental bearing friction torque was greater than that predicted by theory, but it was within twice the theoretical amount. The resulting lower experimental film thickness could account for greater friction torque.

Lewis Research Center,
National Aeronautics and Space Administration,
Cleveland, Ohio, December 18, 1978,
505-04.

REFERENCES

1. Licht, L.: Foil Bearings for Axial and Radial Support of High Speed Rotors: Design, Development, and Determination of Operating Characteristics. NASA CR-2940, 1978.

2. Barnett, M. A.; and Silver, A.: Application of Air Bearings to High-Speed Turbomachinery. SAE Paper 700720, Sep. 1970.

3. Licht, L.; Branger, M.; and Anderson, W. J.: Gas-Lubricated Foil Bearings for High Speed Turboalternator - Construction and Performance. J. Lubr. Technol., vol. 96, no. 2, Apr. 1974, pp. 215-223.

4. Walowitt, J. A.; et al.: Gas Lubricated Foil Bearing Technology Development for Propulsion and Power Systems. MTI-73TR37, Mechanical Technology, Inc., 1973 (AFAPL-TR-73-92, AD-774024.)

5. Nemeth, Z. N.: Experimental Evaluation of Foil-Supported Resilient-Pad Gas-Lubricated Thrust Bearing. NASA TP-1030, 1977.

6. Etsion, I.; and Fleming, D. P.: An Accurate Solution of the Gas-Lubricated, Flat Sector Thrust Bearing. J. Lubr. Technol., vol. 99, no. 1, 1977, pp. 82-88.

7. Oser, J.: Ein hydrodynamisches Axiallager mit elastischen Gleitflaechen (Hydrodynamic Thrust Bearing with Elastic Pads). Konstrucktion Masch. Appar Geraetebau, vol. 23, no. 9, Sep. 1971, pp. 344-351.

8. Etsion, I.: A Cantilever Mounted Resilient Pad Gas Thrust Bearing, J. Lubr. Technol., vol. 99, no. 1, 1977, pp. 95-100.

9. Nemeth, Zolton N.: Evaluation of Chromium Oxide and Molybdenum Disulfide Coatings in Self-Acting Stops of an Air-Lubricated Rayleigh Step Thrust Bearing. NASA TN D-7656, 1974.

10. Halling, J., ed.: Principles of Tribology. MacMillan & Co., Ltd. (London), 1975.

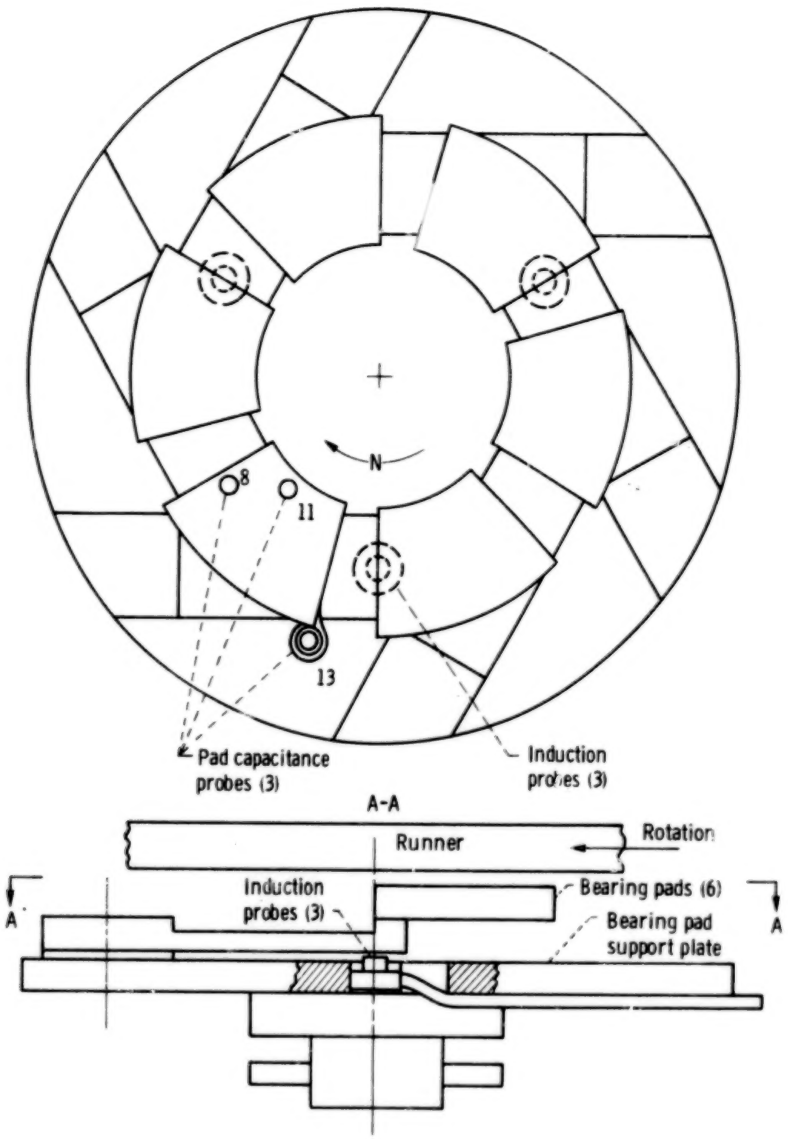

Figure 1. - Schematic of cantilever-mounted multipad thrust bearing.

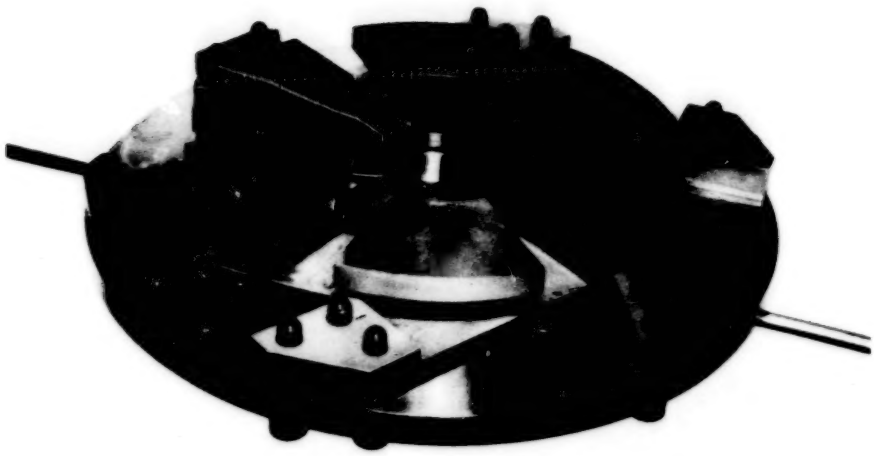

(a) Stator.

(b) Runner.

Figure 2. - Cantilever-mounted-pad thrust bearing.

(a) Front view.

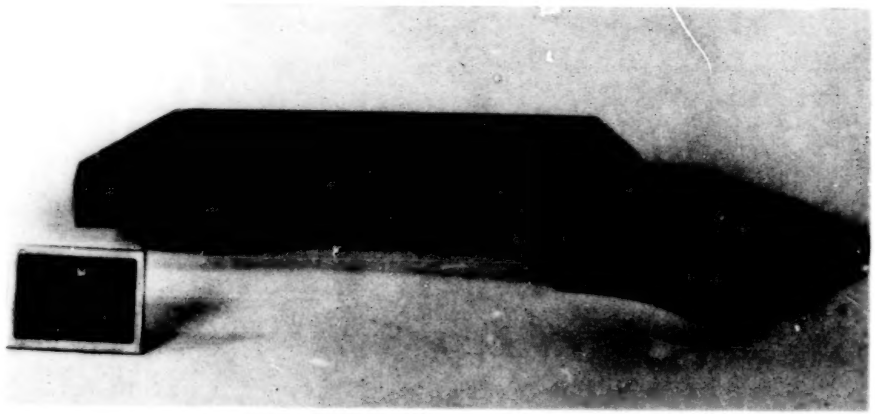

(b) Back view.

Figure 3. - Cantilever-mounted pad.

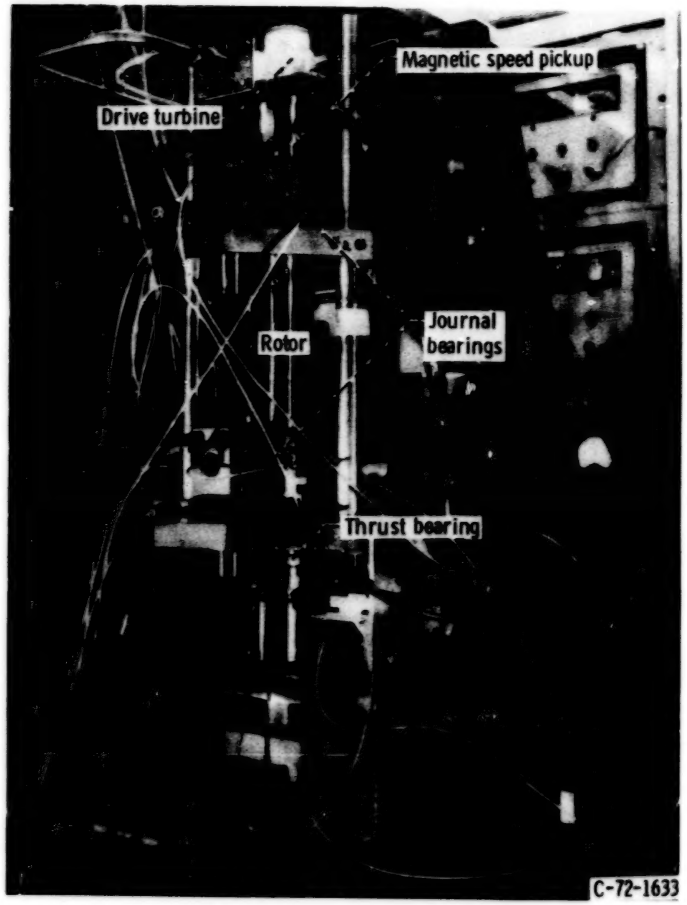

Figure 4. - Thrust bearing test apparatus.

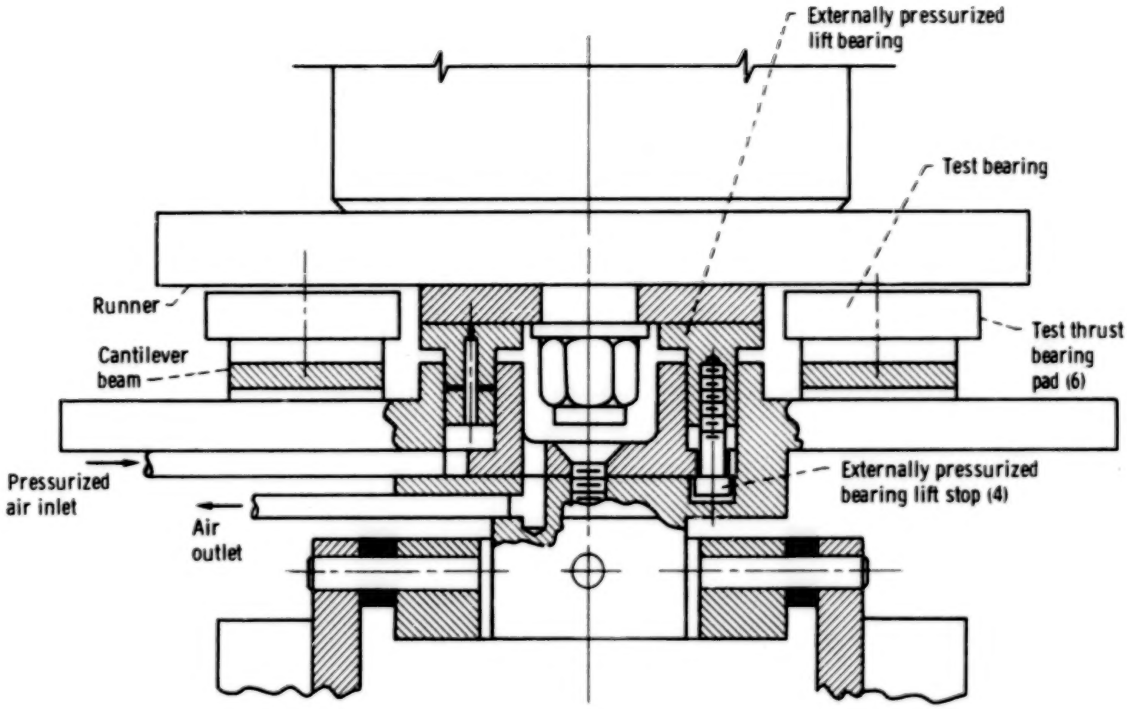

Figure 5. - Schematic of externally pressurized shaft lift bearing for startup and shutdown.

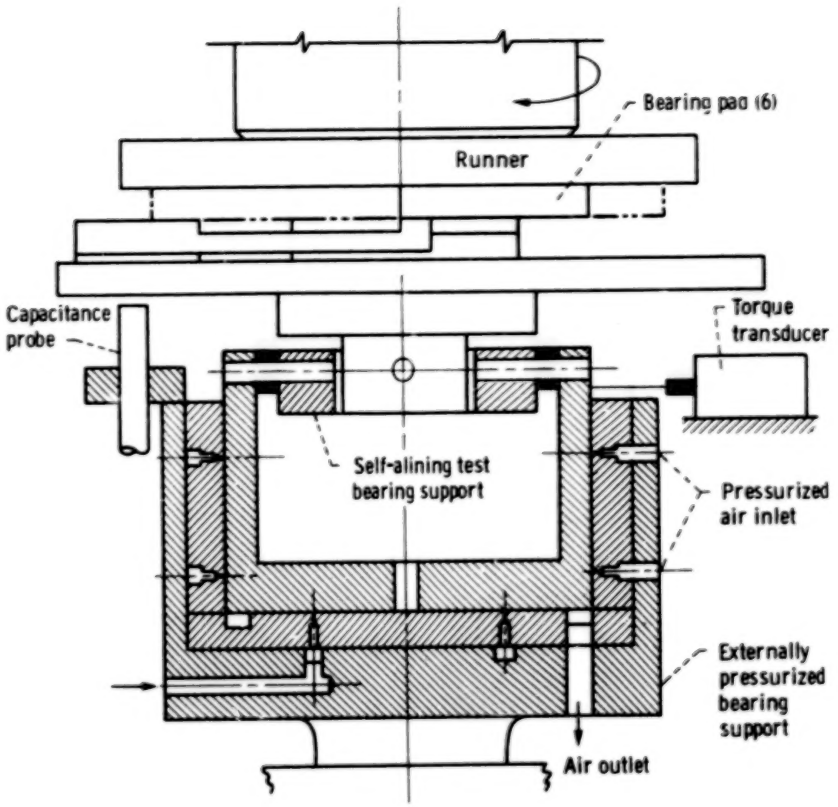

Figure 6. - Schematic of thrust bearing self-alining and frictionless externally pressurized support.

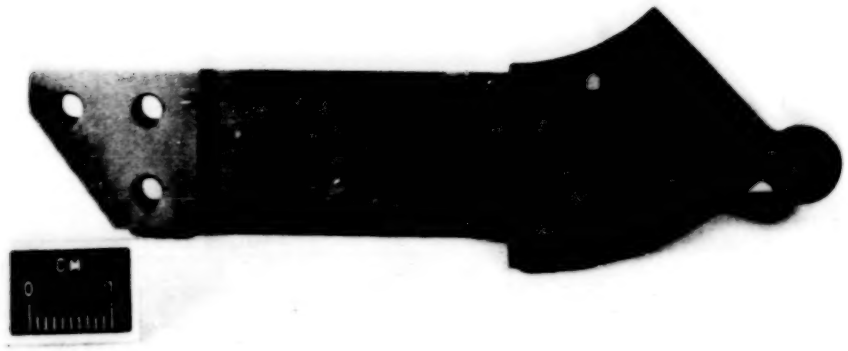

(a) Surface of pad.

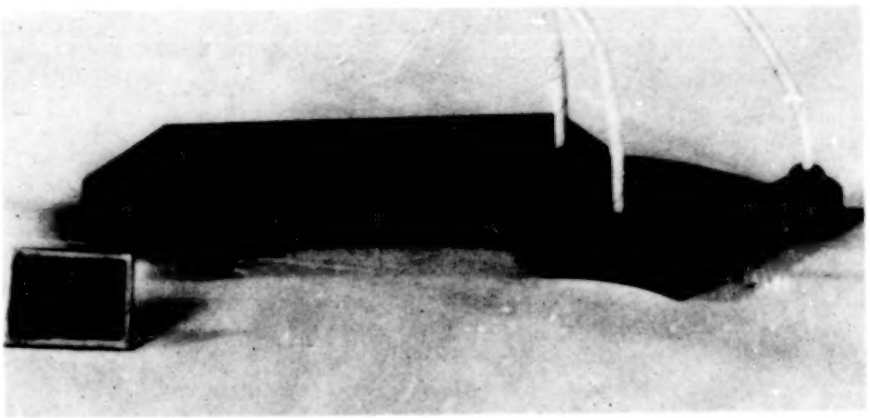

(b) Back of pad.

Figure 7. - Cantilever-mounted pad showing instrumentation for film thickness measurement.

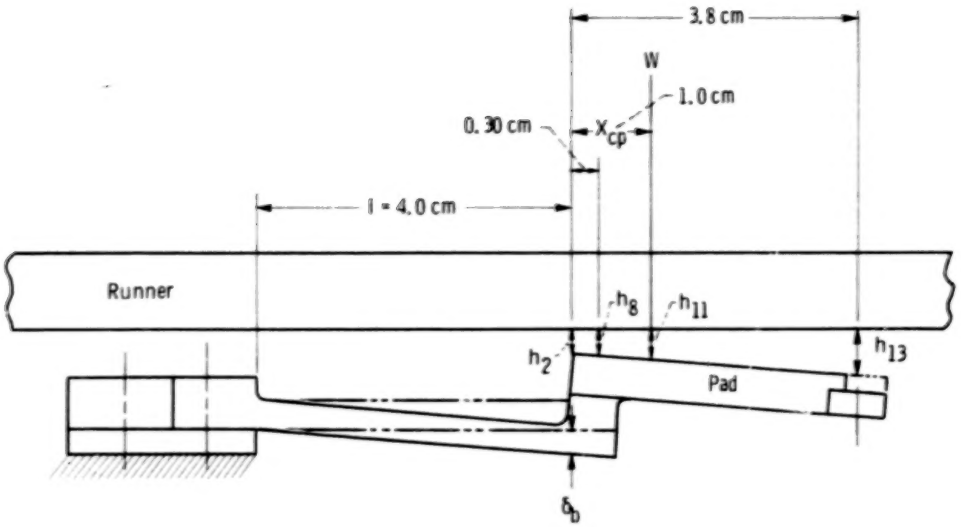

Figure 8. - Schematic of cantilever-mounted pad showing probe locations.

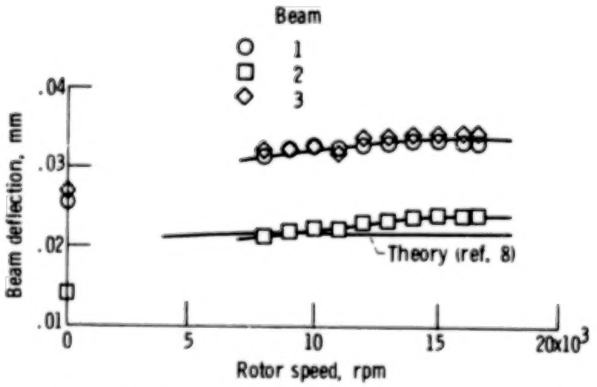

Figure 9. - Beam deflection at trailing edge of pad as function of shaft speed.

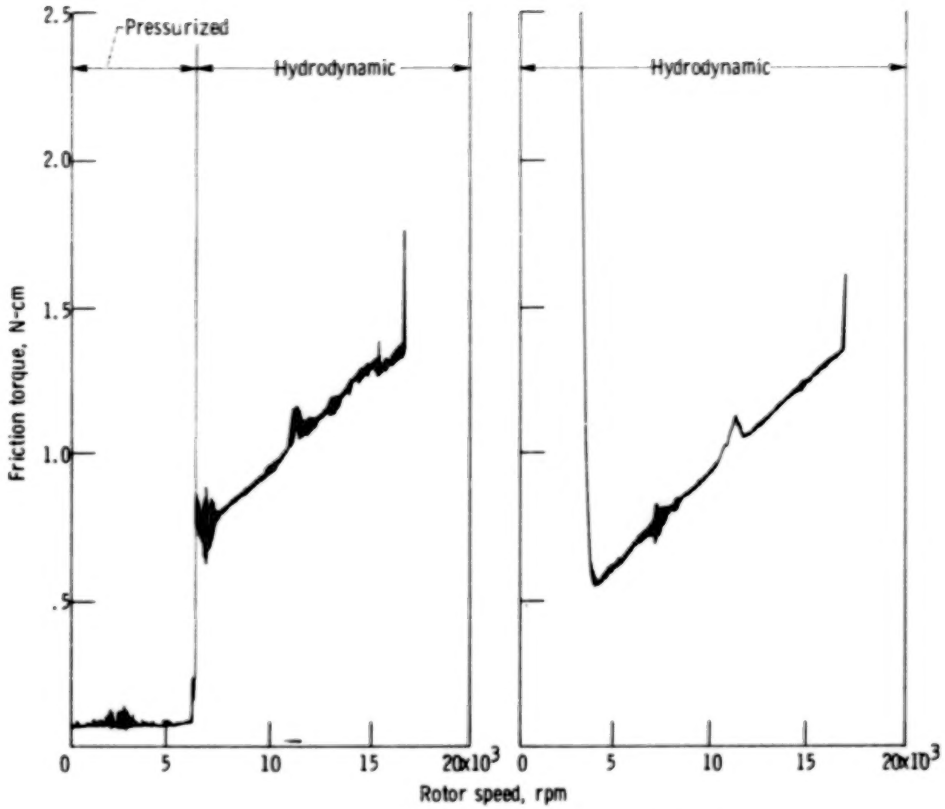

(a) Increasing speed.

(b) Coastdown.

Figure 10. - Friction torque as function of rotor speed. Thrust bearing; assembly 1; self-aligning bearing mount.

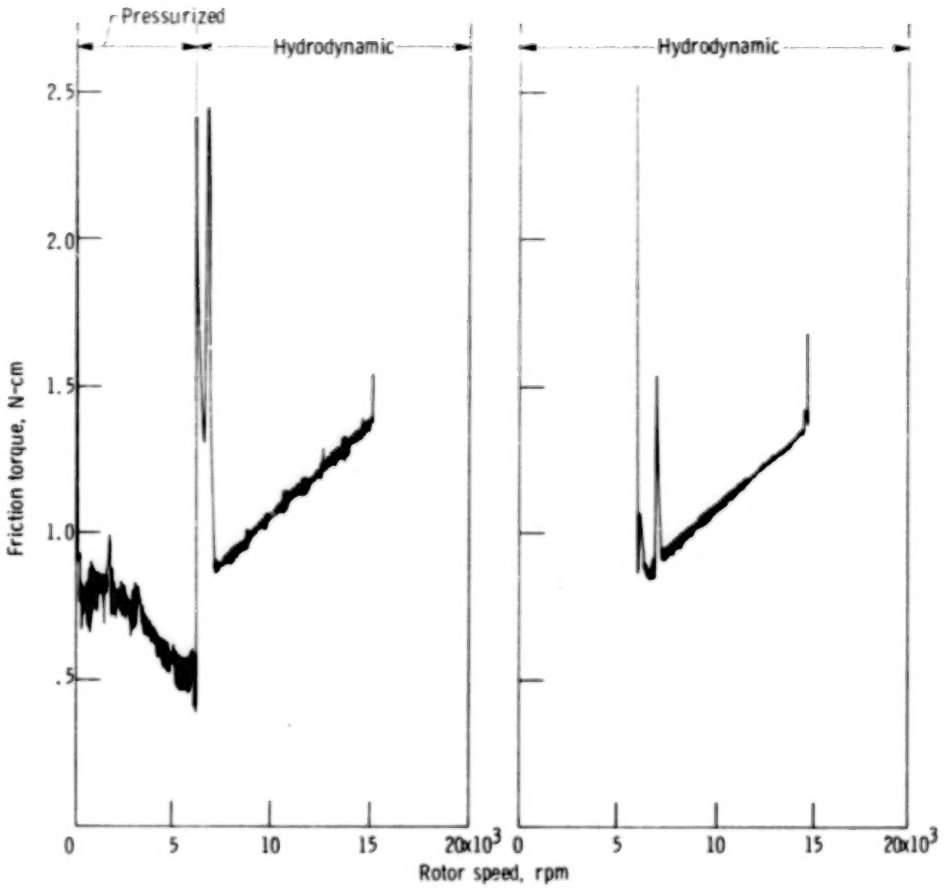

(a) Increasing speed.

(b) Coastdown.

Figure 11. - Friction torque as function of rotor speed. Thrust bearing; assembly 2; clamped bearing mount.

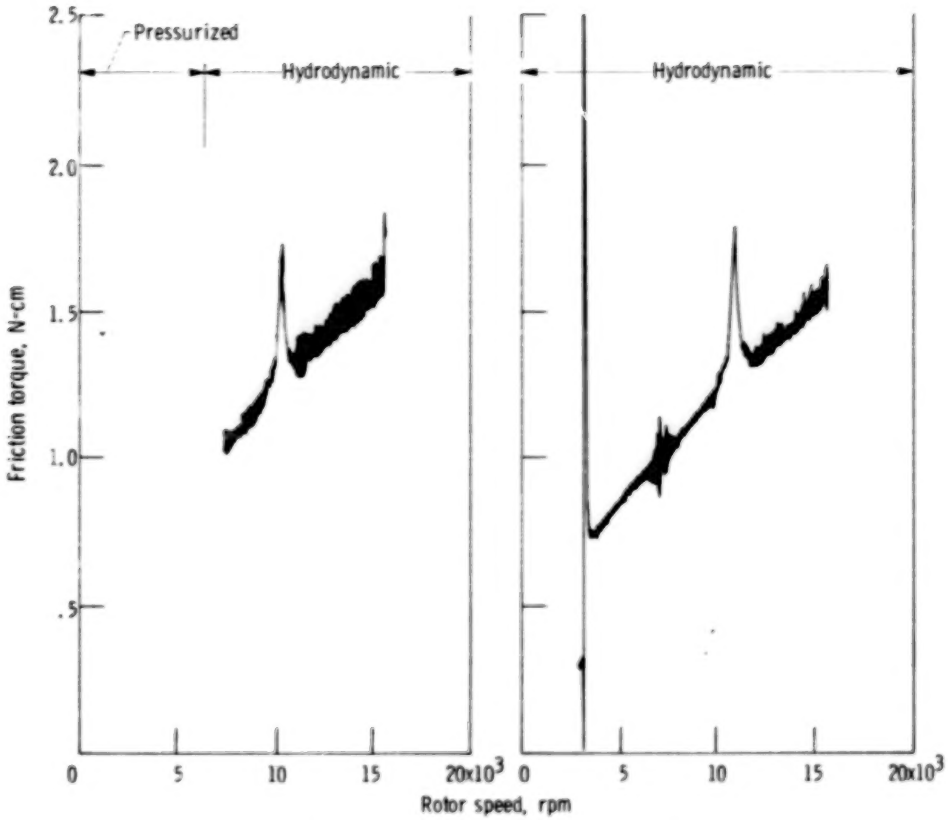

(a) Increasing speed. (b) Coastdown.

Figure 12. - Friction torque as function of rotor speed. Thrust bearing, assembly 3; run 3; self-aligning gimbal bearing mount.

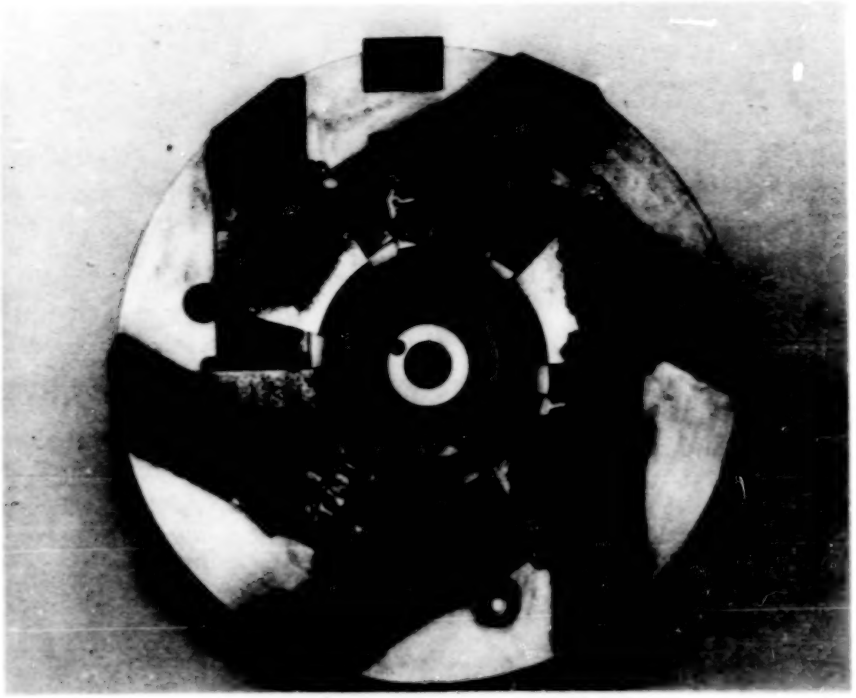

Figure 13. - Thrust bearing after test. Second assembly, clamped bearing mount.

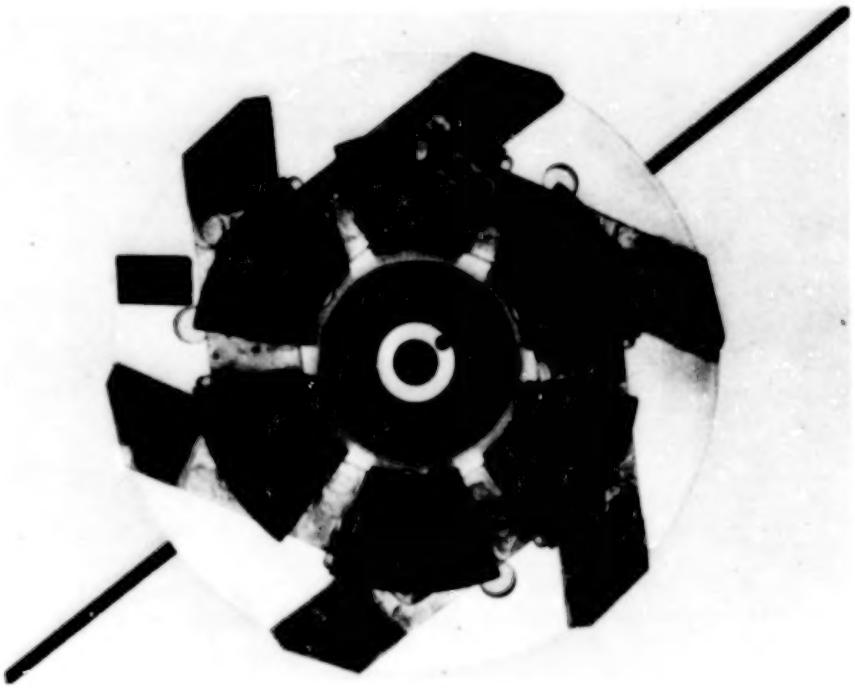

Figure 14. - Thrust bearing before test. First assembly.

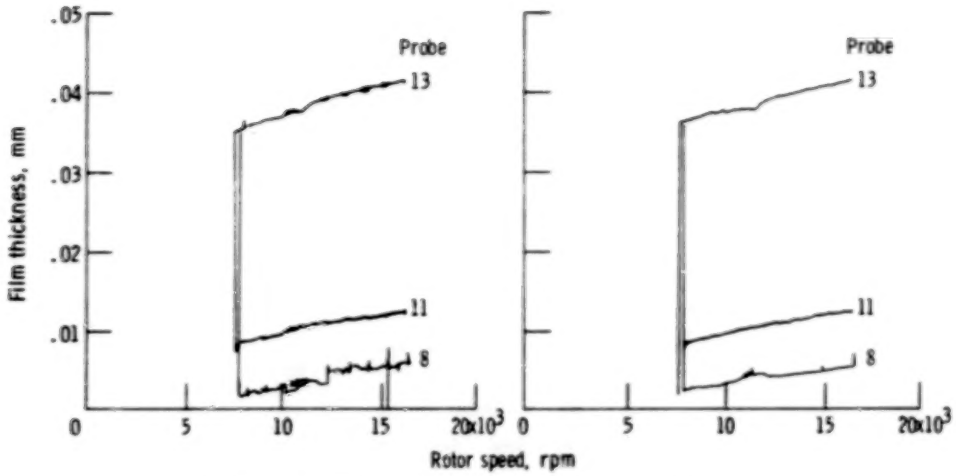

Figure 15. - Pad clearance as function of rotor speed. Thrust bearing; assembly 3; run 1; gimbal self-alining bearing mount.

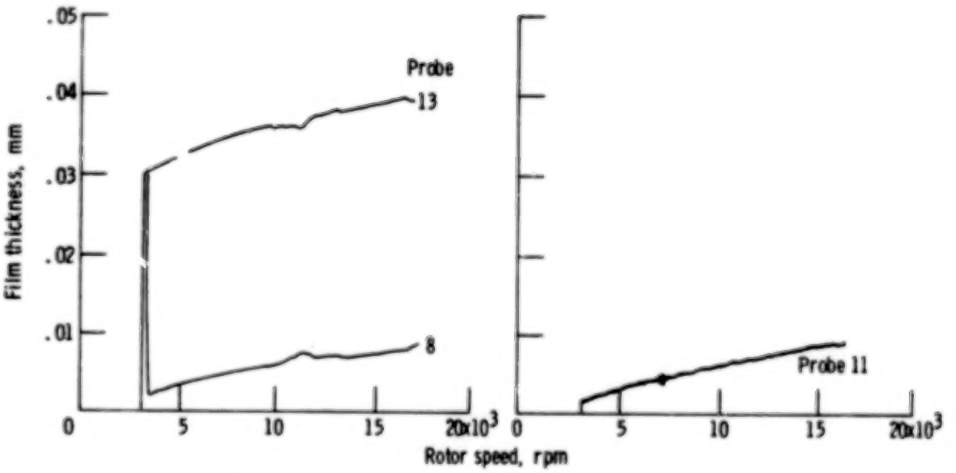

Figure 16. - Pad clearance as function of rotor speed. Thrust bearing; assembly 3; run 2; coastdown in speed; gimbal self-alining bearing mount.

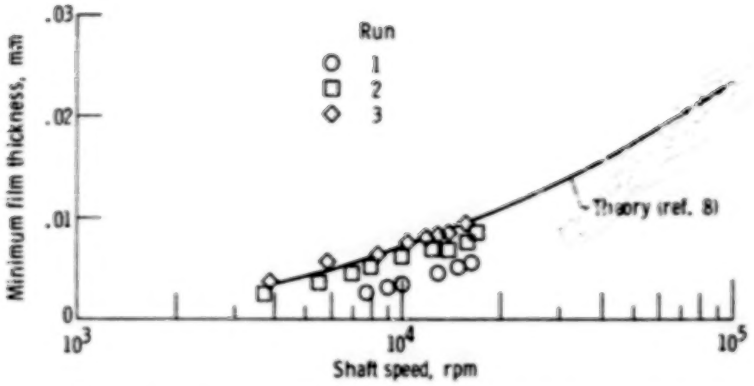

Figure 17. - Minimum film thickness as function of shaft speed. Comparison of experimental data with theory. Thrust bearing, assembly 3, three runs.

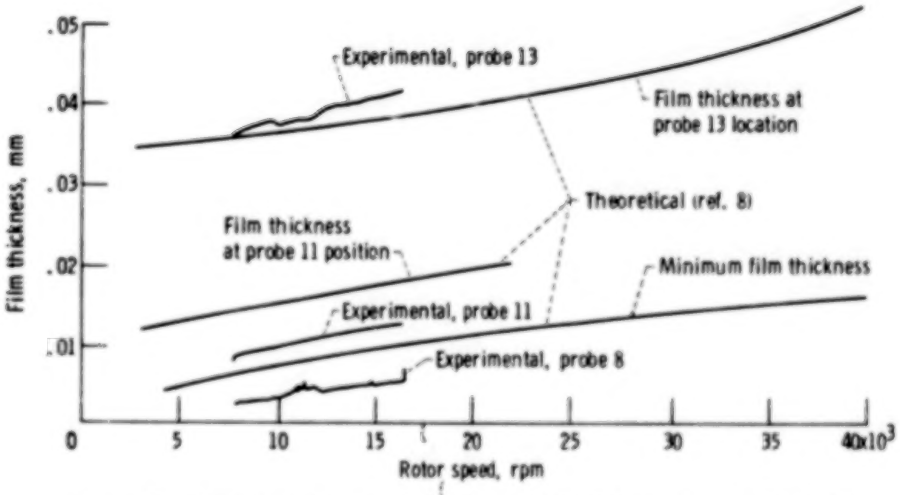

Figure 18. - Comparison of experimental and theoretical pad clearance as function of rotor speed. Thrust bearing, assembly 3, run 1.

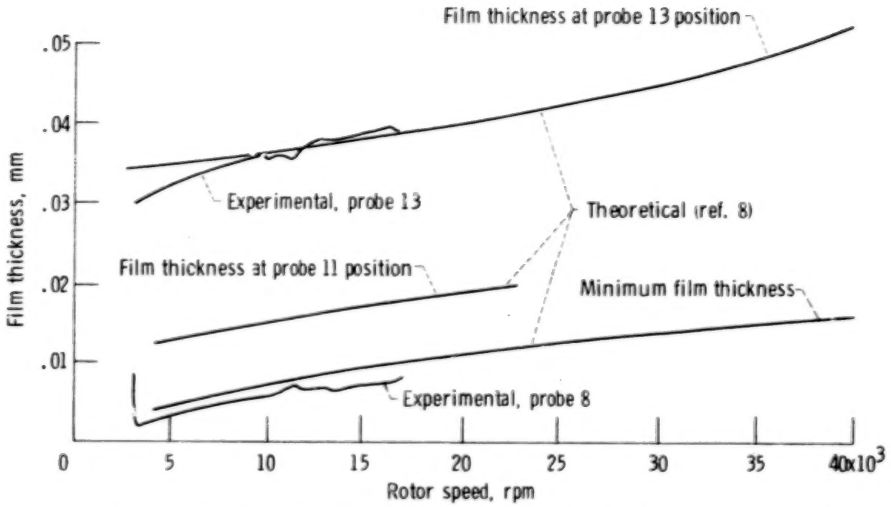

Figure 19. - Comparison of experimental and theoretical pad clearance as function of rotor speed. Thrust bearing, assembly 3, run 2.

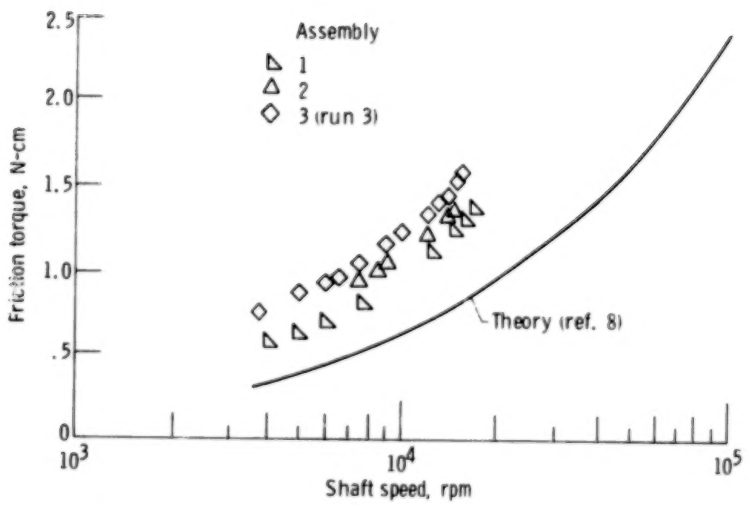

Figure 20. - Friction torque as function of shaft speed for cantilever-mounted resilient-pad gas thrust bearing.

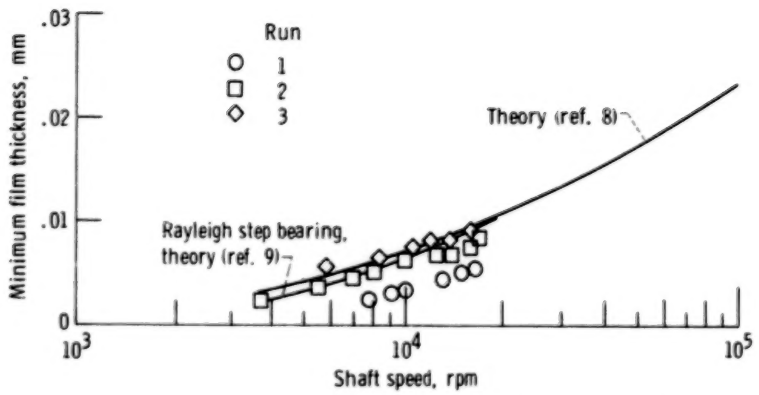

Figure 21. - Minimum film thickness as function of shaft speed. Comparison of experimental data with theory for thrust bearing assembly 3 with Rayleigh step thrust bearing.

1. Report No.	2. Government Accession No.	3. Recipient's Catalog No.
NASA TP-1438		

4. Title and Subtitle	5. Report Date
OPERATING CHARACTERISTICS OF A CANTILEVER-MOUNTED RESILIENT-PAD GAS-LUBRICATED THRUST BEARING	April 1979
	6. Performing Organization Code
7. Author(s)	8. Performing Organization Report No.
Zolton N. Nemeth	E-9815
	10. Work Unit No.
9. Performing Organization Name and Address	505-04
National Aeronautics and Space Administration Lewis Research Center Cleveland, Ohio 44135	11. Contract or Grant No.
	13. Type of Report and Period Covered
12. Sponsoring Agency Name and Address	Technical Paper
National Aeronautics and Space Administration Washington, D.C. 20546	14. Sponsoring Agency Code

15. Supplementary Notes

16. Abstract

A resilient-pad gas thrust bearing consisting of pads mounted on cantilever beams was tested to determine its operating characteristic. The bearing was run at a thrust load of 74 newtons to a speed of 17 000 rpm. The pad film thickness and bearing friction torque were measured and compared with theory. The measured film thickness was less than that predicted by theory. The bearing friction torque was greater than that predicted by theory.

17. Key Words (Suggested by Author(s))	18. Distribution Statement
Bearings Gas bearings Thrust bearings Compliant bearings	Unclassified - unlimited STAR Category 37

19. Security Classif. (of this report)	20. Security Classif. (of this page)	21. No. of Pages	22. Price*
Unclassified	Unclassified	29	A03

* For sale by the National Technical Information Service, Springfield, Virginia 22161

NASA-Langley, 1979

END

September 11, 1979